Am J Nucl Med Mol Imaging 2023;13(6):269-278
www.ajnmmi.us /ISSN:2160-8407/ajnmmi0152565

Original Article

Diagnosis and prognostic predictive value of delineation methods from ^{18}F-FDG PET/CT and PET/MR in pancreatic lesion

Fan Hu[1,2*], Xiao Zhang[1,2*], Hua Shu[1,2], Xiaoli Wang[1,2], Shuqian Feng[1,2], Mengmeng Hu[1,2], Xiaoli Lan[1,2], Chunxia Qin[1,2]

[1]*Department of Nuclear Medicine, Union Hospital, Tongji Medical College, Huazhong University of Science and Technology, Wuhan 430022, Hubei, China;* [2]*Hubei Key Laboratory of Molecular Imaging, Wuhan 430022, Hubei, China.* [*]*Equal contributors.*

Received August 1, 2023; Accepted December 21, 2023; Epub December 25, 2023; Published December 30, 2023

Abstract: The aim was to utilize three segmentation methods on ^{18}F-FDG PET/CT and PET/MR images of pancreatic neoplasm patients, and further compare the effectiveness in differentiating benign from malignant, TNM-stage and prognosis. We conducted a retrospective analysis of 51 patients with pancreatic neoplasm who had undergone ^{18}F-FDG PET/CT and PET/MR before treatment. The patients were categorized into malignant and benign groups. For each patient, the lesion was segmented by 3 thresholds and we recorded TNM-stage, treatment strategy, time to death, and the performance status of survivors. We used receiver operating characteristic (ROC) analysis to compare the diagnostic performance of different threshold delineations between benign and malignant, as well as TNM-stage of adenocarcinoma patients. The optimal model of prognostic value was also assessed by Cox proportional hazards regression analysis and Kaplan-Meier survival analysis. For both PET/CT and PET/MR, SUV_{max} had the best diagnostic efficacy in identifying malignant tumors. The background method of PET/MR exhibited the outstanding performance in M-stage (sensitivity/specificity, 92.90%/88.20%), with the weighted factor being whole-body total lesion glycolysis (WBTLG). In multivariate analysis, WBTLG (Exp [B] = 1.009; P = 0.009), and surgery (Exp [B] = 15.542; P = 0.008) were independent predictive factors associated with prognosis. This study found that SUV_{max} from PET/CT had the best diagnostic efficacy in identifying malignancy, while PET/MR showed higher specificity and accuracy for M-stage. The treatment strategy and WBTLG were independent prognostic factors in pancreatic neoplasm patients. PET/MR using the background method was identified as the optimal predictive model for prognosis.

Keywords: PET/MR, ^{18}F-FDG, pancreatic cancer, segmentation

Introduction

Pancreatic cancer, one of the most lethal malignancies in the world, is characterized by chemoradiotherapy resistance and poor survival [1, 2]. Patients experience an insidious onset and only get mild symptoms [3], resembling common symptoms in the elderly, even as the condition progressed to an advanced stage. So pancreatic cancer is also known as a "silent killer" [4]. Only 10%-15% of pancreatic cancer patients have surgical indications [5]. Despite improvements in the standard of treatment, patients still have a poor prognosis, with a 5-year survival rate of 9% [6]. A critical challenge in clinical practice for patients with pancreatic cancer is the accurate differentiation between malignant and benign lesions in early evaluation [7]. Furthermore, the precise staging of tumor significantly impacts the therapeutic regimens.

Noninvasive imaging such as ultrasonography, computed tomography (CT), magnetic resonance imaging (MRI) and positron emission tomography (PET), plays a critical role in diagnosis and tumor staging [8]. Especially, as a remarkable functional imaging technique, PET has shown significance in distinguishing between malignant and the benign lesions, as well as staging tumor and assessing therapy response [9]. The integration of PET/CT and

PET/MR can provide comprehensive information in a single examination. Compared with PET/CT, PET/MR is superior in abdominal diseases due to high anatomical resolution and signal-to-noise ratio of soft tissue [10, 11]. More importantly, it provides a more sensitive detector (with SiPM, when compared with traditional PET/CT) and acquires bimodal images simultaneously [9], which appears to make it a promising tool in clinical practice.

Quantitative analysis is crucial for the comprehensive assessment of ^{18}F-FDG PET images, in addition to visual inspection. The maximum standardized uptake value (SUV_{max}) served as a vital indicator for differentiating benign from malignant tumors, as well as for predicting the therapeutic response and prognosis of some cancer patients [12]. However, the limitation of this parameter lies in its ignorance of tumors' integrity and the overall lesion metabolism. When combined with SUV_{mean}, metabolic tumor volume (MTV) and total glycolysis (TLG), which are determined by the metabolic boundary of the tumor largely, can significantly reflect the metabolic characteristics of the tumor and the overall burden of the patient [13]. The utilization of MTV and TLG plays an essential role in determining the aggressiveness of metabolical active lesions and tumors [14].

Different segmentation methods of PET signals result in different ROI, SUV_{mean}, MTV and TLG. To date, the relative, background-related relative, and absolute thresholds have been widely applied in lesion segmentation [15]. Among them, Th 40 is a widely used relative threshold segment method, which delineates the targeted tissue as all voxels within the lesion with a SUV > 40% SUV_{max} of the lesion. The background-related relative threshold takes the surrounding background into the volume calculation of the target tissue. An absolute threshold, SUV_{max} > 2.5, on ^{18}F-FDG PET/CT has been widely adopted as a cutoff value for distinguishing between malignant and benign diseases [16]. The use of 3 threshold delineation methods has been extensively discussed in PET/CT [17-19], while being rarely investigated in PET/MR.

Here, we utilized the segmentation methods (Th 40, background and SUV 2.5 thresholds) in PET/MR images of pancreatic neoplasm, and compared them with PET/CT images. Additionally, we conducted further analysis to differentiate benign from malignant lesions, as well as to assess T stage, M stage and prognosis.

Patients and methods

Patients

The study was approved by the Institutional Review Board of our hospital. We conducted a retrospective analysis of imaging data of all patients diagnosed with pancreatic neoplasm who underwent ^{18}F-FDG PET/CT and PET/MR at Union Hospital, Tongji Medical College, Huazhong University of Science and Technology, from November 2017 to November 2019. Inclusion criteria were as follows: (1) Age ≥ 18 years; (2) Pancreatic neoplasms were observed on PET/CT or PET/MR; (3) Complete clinical and imaging data; (4) The patients finished both PET/CT and PET/MR scans before treatment. Patients who had already commenced treatment before the PET scan, and those lost to follow-up were excluded. The cases were divided into malignant and benign groups according to the histological or follow-up results. For the patients with adenocarcinoma, we recorded the therapeutic regimen (including surgery, chemoradiotherapy, or palliative treatment), TNM stage, time to death, and performance status of survivors. Overall survival (OS) was defined as the time interval from the date of PET/CT and PET/MR scan to pancreatic tumor-related death. The follow-up period of adenocarcinoma patients was 7.02±4.79 months (ranged from 1 to 26 months). Patients' death time served as the endpoint of follow-up.

^{18}F-FDG PET/CT and PET/MR protocol

^{18}F-FDG was synthesized with ^{18}F produced by a cyclotron (MINItrace®, GE Healthcare, Milwaukee, WI, USA), with radiochemical purity > 95%. All patients fasted for at least 8 h before the examination of ^{18}F-FDG PET/CT and PET/MR. An intravenous administration of 3.70-5.55 MBq (0.10-0.15 mCi)/kg ^{18}F-FDG was conducted. PET/CT was performed approximately 60 min after ^{18}F-FDG administration by a PET/CT scanner (Discovery VCT®, GE Healthcare), then followed by PET/MR scans (TOF PET/MR scanner, Singa®, GE Healthcare). Concurrent with the PET acquisition, MR Imaging protocols included T2-fat saturation

images (TR/TE, 9500/93.1 ms; matrix 288 × 256), T2-FSE images (TR/TE, 3750 ms/68 ms; matrix 320 × 256), T1-LAVA-Felx images (TR/TE, 5 ms/1.2 ms; matrix 260 × 192) and diffusion weighted imaging (DWI, TR/TE, 6200 ms/69.5 ms; matrix 128 × 128) with a section thickness of 4 mm and an intersection gap of 1 mm. For PET imaging, the FORE-Iterative reconstruction algorithm with 28 subsets, 2 iterations, and 2.14 mm (full width at half maximum) post-filtering was used.

PET/CT and PET/MR images analysis

PET/CT and PET/MR images were visually interpreted by two experienced nuclear medicine physicians in consensus, with knowledge of the initial clinical data but blinded to the histology. The physicians reviewed the PET, CT and MR images and documented their findings respectively. The CT and MR diagnosis primarily considered the location of the neoplasm (head, neck/body and tail), with/without lymph node metastasis and TNM stage. A semiquantitative approach was applied to the PET interpretation, which was based on several metabolic indices of ^{18}F-FDG uptake (SUV_{max}, SUV_{mean}, MTV and TLG). All PET/CT and PET/MR data were processed in DICOM format using Advanced Workstation (AW, GE Healthcare). The lesions were identified on PET images and segmented automatically using a 3D-area growing algorithm. The regions of interest (ROIs) identified from PET were copied to the synchronous MR images to obtain the minimum apparent diffusion coefficient value (ADC_{min}) and the maximum exponential apparent diffusion coefficient value ($eADC_{max}$).

Three thresholds were selected for PET delineation: (1) The absolute threshold (Th 2.5) was calculated as SUV_{max} = 2.5 marking all voxels inside foci with SUV > 2.5 as target tissues; (2) The relative threshold (Th 40) was calculated as SUV = 40% × SUV_{max}, indicating that all voxels inside the lesion with an SUV > 40% SUV_{max} of the lesion would be labeled as target tissue; (3) The relative background dependent threshold (Th bgd) was calculated as SUV = SUV_{bgd} + 20% (SUV_{max} - SUV_{bgd}). The volume and SUV_{mean} of each lesion were calculated by AW. The MTV of each slice was then calculated by multiplying the area within the threshold margin. WBMTV was the sum of all MTVs from one patient. TLG was calculated as multiplying the MTV by the SUV_{mean}. The sum of the TLGs of each lesion was the whole-body TLG (WBTLG).

Statistical analysis

SPSS 22.0 (IBM Inc., Armonk, NY, USA) was used for data processing. Continuous variables were presented as mean ± SD. Student's t test was employed for quantitative data with normal distribution and equal variances, while Welch's t test was applied in case of unequal variance. Mann-Whitney U test was utilized to compare between two groups (benign and malignant) with non-normal distribution or categorical variables quantitative data. Receiver operating characteristic (ROC) analysis was used for comparing the different diagnostic performances (SUV_{max}, SUV_{mean}, MTV, TLG, WBMTV, WBTLG, ADC and eADC value) between benign and malignant of each threshold delineation model, as well as TNM stage. The optimal cut-off value was determined as the point with the highest sum of sensitivity and specificity. Multi-factor ROC analysis was performed after single factor ROC analysis, while logistic regression was used to construct the measurement model and ascertain the weight of each variable. For adenocarcinoma patients, univariate analysis included the effects of age, gender, tumor location, TNM stage, SUV_{max}, SUV_{mean}, WBMTV, WBTLG, and different therapy methods. The Cox proportional hazards model was used to assess the independent factors influencing OS.

Results

The final study population consisted of 51 patients (34 males, 17 females; 57.84±14.54 years). The pancreatic neoplasms were diagnosed as follows: (1) Malignancy = 38 (74.51%; adenocarcinoma [n = 32], intraductal papillary-mucinous carcinoma [n = 1], mucinous cystadenocarcinoma [n = 1], malignant endocrine tumor [n = 2], metastatic lesion [n = 2]); (2) Benign = 13 (25.49%). The clinical characteristics of the patients were presented in **Table 1**.

Different threshold methods resulted in different ROIs, which could lead to relative differences in SUV_{mean}, MTV and TLG. **Figure 1** illustrated three delineation methods from ^{18}F-FDG PET/CT and PET/MR in pancreatic lesion. PET/MR images (**Figure 1A-C**) showed higher SUV compared to PET/CT images (**Figure 1D-F**). ROIs identified from PET were copied to DWI images, obtained different ADC and eADC val-

Table 1. Clinical information of the patients with pancreatic neoplasms

Category	Total
Age (years)	57.84±14.54
Gender (M/F)	34/17
Malignant	38
Adenocarcinoma	32[a]
Intraductal papillary-mucinous carcinoma	1
Mucinous cyst-adenocarcinoma	1
Malignant endocrine tumor	2
Metastatic tumor	2
Benign	13
Pancreatitis	3
Pancreatic tissue	2
Tuberculosis	1
Serous cyst adenoma	3
other	4

[a]One of these cases is adenosquamous carcinoma.

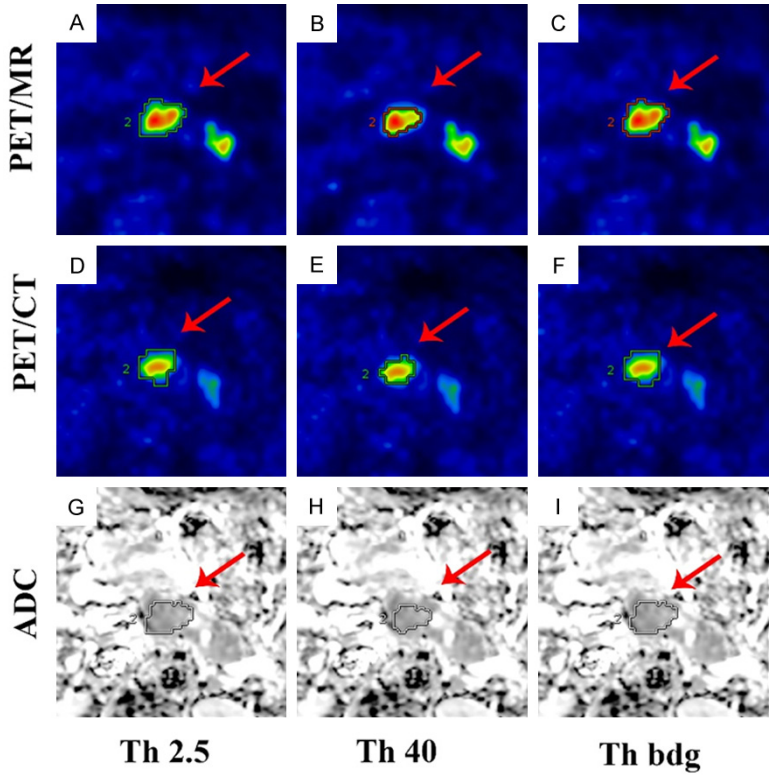

Figure 1. Three delineation methods of ^{18}F-FDG PET/CT and PET/MR in pancreatic lesion. PET/MR images (A-C) showed higher SUV compared to the lesion in PET/CT images (D-F). ROIs identified from PET were copied to DWI images (G-I). The ROI of the lesion varied with the delineation methods.

ues (**Figure 1G-I**). The ROI of the lesion varied with the delineation methods.

Diagnostic performance in pancreatic lesion

The PET characteristics of PET/CT and PET/MR between benign and malignant groups were outlined in **Table 2**. The analysis indicated that SUV_{max} and SUV_{mean} from different threshold methods were all significant in distinguishing between benign and malignancy. A multi-factor ROC analysis was conducted to compare the efficacy of three threshold delineation methods in diagnosing pancreatic lesions (benign or malignant, **Figure 2A**). On both PET/CT and PET/MR, SUV_{max}, identified as the most weighted factor by logistic regression, presented highest diagnostic accuracy in identifying benign patients (cutoff value of PET/CT, 3.55, 92.30%/91.60% [sensitivity/specificity]; cutoff value of PET/MR, 6.05, 84.80%/86.80% [sensitivity/specificity]). Linear and quadratic regression equations were used to evaluated for correlations between PET/CT and PET/MR parameters (SUV_{max} and TLG, **Figure 2C** and **2D**). For the SUV_{max} value, the linear regression equation parameters and percentage of variance accounted for R^2 were $y = 0.681x + 0.481$ and adjusted $R^2 = 0.688$ ($P < 0.01$), respectively. For the TLG value, the linear regression equation was $y = 0.267x + 0.01x^2 + 26.257$ and adjusted $R^2 = 0.971$ ($P < 0.01$; **Figure 2D**).

Diagnostic performance in T-stage and M-stage

Out of the 32 patients with pancreatic adenocarcinomas, 18 didn't have distant metastasis,

Table 2. PET indices of different threshold methods among benign and malignant groups

Groups		Benign (n = 13)	Malignant (n = 38)	*P* value
Age (years)		50.23±11.41	60.45±14.70	0.027
Gender (M/F)		10/3	24/14	0.502
PET/CT	SUV_{max}	3.3±2.54	6.33±3.22	0.003
Th 40	SUV_{mean}	1.80±1.40	3.55±1.90	0.004
	MTV	11.49±8.80	18.87±20.95	0.225
	TLG	28.55±52.75	86.98±152.35	0.184
Th bgd	SUV_{mean}	1.75±1.06	3.05±1.40	0.004
	MTV	12.06±14.78	28.08±31.30	0.083
	TLG	34.19±78.64	115.42±201.24	0.164
Th 2.5	SUV_{mean}	1.86±1.63	3.55±0.92	0.003
	MTV	5.40±18.67	21.81±37.53	0.138
	TLG	25.20±88.58	105.71±223.80	0.215
PET/MR	SUV_{max}	4.33±3.99	8.50±3.57	0.001
Th 40	SUV_{mean}	2.50±2.18	4.85±2.07	0.001
	MTV	11.54±9.34	17.91±25.41	0.384
	TLG	39.44±74.84	97.22±176.29	0.259
	ADC_{min} (m^2/s)	0.52±0.36	0.45±0.42	0.614
	$eADC_{max}$	0.68±0.20	0.73±0.22	0.502
Th bgd	SUV_{mean}	2.39±1.71	4.20±1.61	0.001
	MTV	10.80±12.95	26.24±32.96	0.108
	TLG	44.21±103.78	134.69±211.16	0.146
	ADC_{min}	0.56±0.42	0.36±0.35	0.109
	$eADC_{max}$	0.67±0.22	0.78±0.19	0.122
Th 2.5	SUV_{mean}	2.13±1.99	4.19±1.40	0.000
	MTV	7.12±19.43	35.31±41.55	0.084
	TLG	40.19±125.12	138.89±226.18	0.142
	ADC_{min}	0.64±0.32	0.42±0.40	0.152
	$eADC_{max}$	0.62±0.17	0.75±0.21	0.115

while 14 were found to have distant metastases. 32 patients had a total of 69 malignant lesions, which were identified by the following surgical pathology. PET/MR discovered 67 lesions, while PET/CT detected 59 lesions.

There were statistically significant differences in SUV_{mean}, SUV_{max}, WBTLG and MTV between M-stage using three thresholds of PET/CT and PET/MR ($P < 0.05$). Multi-factor ROC analysis was also conducted to compare the efficacy of the three threshold delineation methods in M-stage (**Figure 2B**). PET/CT using background method showed the best diagnostic performance (sensitivity/specificity, 92.90%/100%, **Table 3**) in identifying T-stage (T1 vs. T4). PET/MR using background method demonstrated the best diagnostic performance (sensitivity/specificity, 92.90%/88.20%, **Table 3**) in identifying M-stage. Logistic regression indicated that the most weighted factor was WBTLG.

Follow-up and survival analysis

Surgery with/without adjuvant chemotherapy was the primary therapy for patients with pancreatic adenocarcinomas. Out of 32 pancreatic adenocarcinomas, 10 patients underwent surgery, 17 patients received chemoradiotherapy, and 4 underwent palliative treatment. Over the course of the study, 22 patients passed away and the median survival time was 8.37±1.29 months. A cox proportional hazards model of OS was constructed to evaluate various factors such as age, gender, therapy method, TNM staging, SUV_{max}, SUV_{mean}, MTV, WBTLG, ADC and eADC as potential predictors of disease progression and survival (1 = death). In multi-fac-

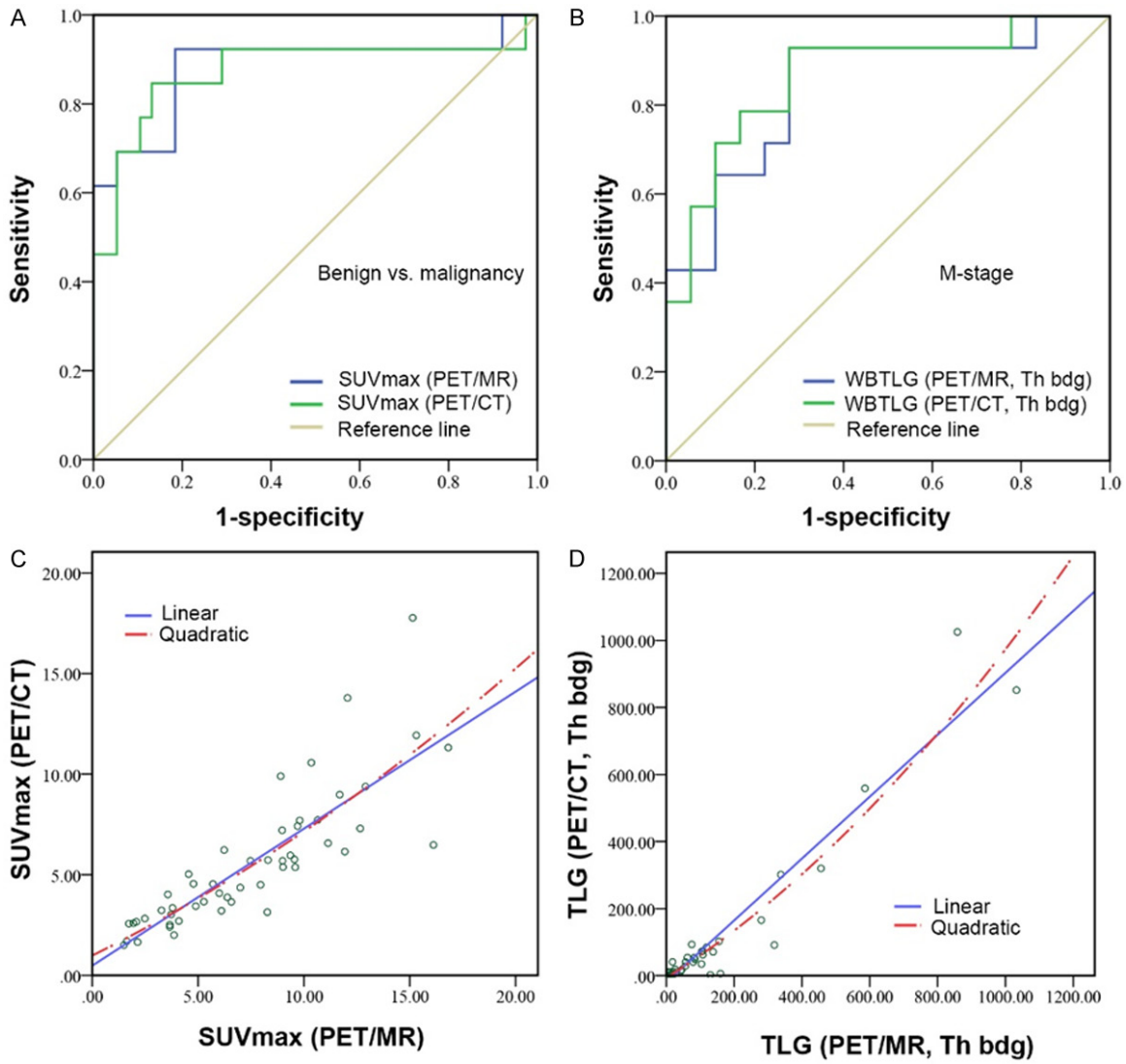

Figure 2. A. The best diagnostic performance of PET/CT and PET/MR in distinguishing benign and malignant with multi-factor ROC analysis; B. The diagnostic performance of PET/CT and PET/MR using Th bgd methods in identifying M-stage from multi-factor ROC analysis; C. The relationship between SUV_{max} from PET/CT and PET/MR; D. The relationship between TLG from PET/CT and PET/MR using Th bgd methods.

tor ROC analysis, the bgd threshold in PET/MR demonstrated the highest efficacy in predicting OS (AUC, 0.850). The weighted factors were WBTLG (Exp [B] = 1.009, P = 0.005), surgery (Exp [B] = 19.918, P = 0.003) and age (Exp [B] = 0.57, P = 0.035) by the cox proportional hazards model (**Table 4**).

Discussion

In this study, the diagnostic efficacy of PET/MR in identifying primary pancreatic lesions was found comparable to that of PET/CT. Perhaps because PET/CT was performed at the most optimal time (1 h after injection), while PETMR was performed much later (1-2 h after injection). Although not statistically significant, PET/MR showed higher specificity and accuracy than PET/CT in M-stage of pancreatic adenocarcinoma patients, particularly when using background methods. Furthermore, it also provided evidence supporting the prognostic value of WBTLG and therapy method in patients with pancreatic adenocarcinoma. Notably, PET/MR using background method showed the best efficacy in predicting the prognosis with an AUC of 0.850. To the best of our knowledge, this is the first report assessing different thresholds of PET/MR images in pancreatic adenocarcinoma.

Table 3. Multi-factor ROC analysis between lesion nature, T-stage and M-stage

Type	Weighted indicator (method)	AUC	*P* value	Sensitivity	Specificity
Benign vs. malignant	SUV_{max} (PET/CT)	0.883	0.000	0.923	0.916
	SUV_{max} (PET/MR)	0.872	0.000	0.848	0.868
T-stage	WBMTV (PET/CT, Th bgd)	0.976	0.001	0.929	1.000
	WBMTV (PET/MR, Th bgd)	0.905	0.005	0.857	1.000
M-stage	WBTLG (PET/CT, Th bgd)	0.882	0.000	0.929	0.824
	WBTLG (PET/MR, Th bgd)	0.887	0.000	0.929	0.882

Table 4. Cox proportional hazards regression analysis of background threshold in PET/MR

Factors	*P* value	Exp (B)	95% CI
Gender	0.054	2.911	0.981-8.638
Age	0.035	0.957	0.918-0.978
Therapy methods	0.006		
Surgery[a]	0.003	19.918	2.794-142.011
Chemoradiotherapy[b]	0.203	3.241	0.530-19.825
M stage	0.223	2.328	0.597-9.077
SUV_{max}	0.066	1.497	0.974-2.300
SUV_{mean}	0.177	0.451	0.142-1.432
WBMTV	0.116	0.968	0.929-1.008
WBTLG	0.005	1.009	1.003-1.016
ADC	0.410	0.009	0.000-699.293
eADC	0.493	0.001	0.000-886745.881

[a]1 = surgery and 0 = not surgery; [b]1 = chemoradiotherapy and 0 = not chemoradiotherapy.

PET/MR imaging is a rapid-developed imaging modality, which integrated high resolution anatomical information and metabolism [20]. There was no obvious difference between PET/CT and PET/MR in identifying the primary pancreatic lesion. Th 40 and background threshold methods showed a higher detection rate of lesions compared to Th 2.5 method. In our previous study, we applied two delineation methods to segment the PET/CT lesions in patients with ovarian cancer [21], which demonstrated that the background threshold method could delineate much more lesions than the SUV 2.5 method. The current study also observed that the threshold of SUV 2.5 left more missed lesions than Th 40 and background methods. There were two potential causes for the inadequate segmentation of the SUV 2.5 method: the omissions of target lesions with an SUV less than 2.5, and the integration of different target lesions and their surrounding tissue with an SUV more than 2.5.

PET/MR showed its superiority in tumor staging [22, 23]. Some PET/CT cases might face challenges in anatomical co-registration, due to the asynchronous acquisition of PET and CT data. Additionally, PET/CT had limitations in soft tissue resolution and signal contrast, which hindered the clearly delineations of lesion boundaries and the evaluation of T stage. The addition of DWI would also improve the diagnostic accuracy of PET/MRI for N stage [24]. As for M stage, the asynchronous acquisition of PET/CT restricted the detection of liver metastasis and peritoneal implantation metastasis, especially in lesions with size < 10 mm [25]. Furthermore, with the improvements of the collimator, PET/MR demonstrated higher detection efficiency compared to conventional PET/CT. And the application of the time-of-flight (TOF) and point-spread function (PSF) had significantly increased the SUV of small lesions in PET/MR images, potentially improving the detectability of small lesions [26]. Here, PET/MR was superior to PET/CT in differentiating M-stage, particularly when using the background method. The advantage of this threshold lay in the calculation of the surrounding background, taking full account of the high FDG uptake area and the surrounding normal tissue, which provided a more precise assessment of target lesions.

In this cohort of pancreatic cancer patients, the median survival time was founded to be 8.37±1.29 months, consistent with findings from other studies [27, 28]. Multivariate analysis identified the treatment strategy and TLG as the independent prognostic factors. Lower TLG was associated with longer survival [29], and surgical treatment could significantly improve the prognosis and survival time of patients with postoperative indications. Background threshold method showed the best overall performance in predicting OS and thus served as an indicator of prognosis.

Several studies had shown that ADC played a crucial role in distinguishing between benign and malignant lesions, as well as in predicting the prognosis of pancreatic cancer patients [30, 31]. Here, the malignant lesions had lower ADC_{min} and higher $eADC_{max}$ while these differences were not found to be statistically significant. Perhaps due to the inaccurate corresponding positions of PET and DWI, the projection of the ROI onto the DWI image according to the outline of PET metabolism, might resulting in the inaccurate acquisition of lesion information on DWI. In the study of Chao et al [32], ADC was also not effective in the differentiating between pancreatic ductal adenocarcinoma and chronic pancreatitis. The ADC_{min} and $eADC_{max}$ values of PET ROI were found to be limited diagnostic and prognostic utility.

Several considerations still remained to be pointed out in our study. An optimal experimental design would involve simultaneous collection of PET/CT and PET/MR, or at least with a minimum scan interval between PET/CT and PET/MR. Texture analysis had been applied to tumor nuclear medicine imaging in recent years. Future research should not only analyze the metabolic parameters such as SUV_{mean}, MTV, TLG etc., but also integrate the outlined ROI with texture analysis to yield more substantive findings. Furthermore, various MR sequences should be collected and analyzed to fully exploit the potential of PET/MR. PET/MR not only offered high-resolution of PET, but also capitalized the superior soft tissue resolution of MR. Local multi-MR sequences should be collected during PET/MR data acquisition to provide more diagnostic values.

Conclusion

SUV_{max} from PET/CT demonstrated superior diagnostic efficacy in detecting malignancy. PET/MR showed higher specificity and accuracy of M-stage. The treatment strategy and WBTLG were identified as independent prognostic factors in patients with pancreatic adenocarcinoma. Utilizing with background method, PET/MR represented an optimal predictive model for prognosis.

Acknowledgements

The authors are grateful for the support from the National Natural Science Foundation of China (No. 81901783 and No. 82372026), Hubei Province Science and Technology Innovation Team ([2022] No. 72) and Key Project of Hubei Province Natural Science Foundation (No. 2021CFA008).

Disclosure of conflict of interest

None.

Address correspondence to: Drs. Chunxia Qin and Xiaoli Lan, Department of Nuclear Medicine, Union Hospital, Tongji Medical College, Huazhong University of Science and Technology, No. 1277 Jiefang Ave, Wuhan 430022, Hubei, China. Tel: +86-27-85353136; E-mail: qin_chunxia@hust.edu.cn (CXQ); xiaoli_lan@hust.edu.cn (XLL)

References

[1] Neoptolemos JP, Kleeff J, Michl P, Costello E, Greenhalf W and Palmer DH. Therapeutic developments in pancreatic cancer: current and future perspectives. Nat Rev Gastroenterol Hepatol 2018; 15: 333-348.

[2] McGuigan A, Kelly P, Turkington RC, Jones C, Coleman HG and McCain RS. Pancreatic cancer: a review of clinical diagnosis, epidemiology, treatment and outcomes. World J Gastroenterol 2018; 24: 4846-4861.

[3] Kamisawa T, Wood LD, Itoi T and Takaori K. Pancreatic cancer. Lancet 2016; 388: 73-85.

[4] Kalubowilage M, Covarrubias-Zambrano O, Malalasekera AP, Wendel SO, Wang H, Yapa AS, Chlebanowski L, Toledo Y, Ortega R, Janik KE, Shrestha TB, Culbertson CT, Kasi A, Williamson S, Troyer DL and Bossmann SH. Early detection of pancreatic cancers in liquid biopsies by ultrasensitive fluorescence nanobiosensors. Nanomedicine 2018; 14: 1823-1832.

[5] Parkin A, Man J, Chou A, Nagrial AM, Samra J, Gill AJ, Timpson P and Pajic M. The evolving understanding of the molecular and therapeutic landscape of pancreatic ductal adenocarcinoma. Diseases 2018; 6: 103.

[6] Siegel RL, Miller KD and Jemal A. Cancer statistics, 2020. CA Cancer J Clin 2020; 70: 7-30.

[7] Zhang L, Sanagapalli S and Stoita A. Challenges in diagnosis of pancreatic cancer. World J Gastroenterol 2018; 24: 2047-2060.

[8] Chu LC, Goggins MG and Fishman EK. Diagnosis and detection of pancreatic cancer. Cancer J 2017; 23: 333-342.

[9] Musafargani S, Ghosh KK, Mishra S, Mahalakshmi P, Padmanabhan P and Gulyás B. PET/MRI: a frontier in era of complementary hybrid imaging. Eur J Hybrid Imaging 2018; 2: 12.

[10] Herzog H and Lerche C. Advances in clinical PET/MRI instrumentation. PET Clin 2016; 11: 95-103.
[11] Li Y, Beiderwellen K, Nensa F, Grüneisen J, Dobos G, Herrmann K, Lauenstein T, Umutlu L and Langhorst J. [(18)F]FDG PET/MR enterography for the assessment of inflammatory activity in Crohn's disease: comparison of different MRI and PET parameters. Eur J Nucl Med Mol Imaging 2018; 45: 1382-1393.
[12] Erdogan M, Erdemoglu E, Evrimler Ş, Hanedan C and Şengül SS. Prognostic value of metabolic tumor volume and total lesion glycolysis assessed by 18F-FDG PET/CT in endometrial cancer. Nucl Med Commun 2019; 40: 1099-1104.
[13] Albano D, Bosio G, Treglia G, Giubbini R and Bertagna F. 18F-FDG PET/CT in solitary plasmacytoma: metabolic behavior and progression to multiple myeloma. Eur J Nucl Med Mol Imaging 2018; 45: 77-84.
[14] Albano D, Bosio G, Pagani C, Re A, Tucci A, Giubbini R and Bertagna F. Prognostic role of baseline 18F-FDG PET/CT metabolic parameters in Burkitt lymphoma. Eur J Nucl Med Mol Imaging 2019; 46: 87-96.
[15] Hatt M, Lee JA, Schmidtlein CR, Naqa IE, Caldwell C, De Bernardi E, Lu W, Das S, Geets X, Gregoire V, Jeraj R, MacManus MP, Mawlawi OR, Nestle U, Pugachev AB, Schöder H, Shepherd T, Spezi E, Visvikis D, Zaidi H and Kirov AS. Classification and evaluation strategies of auto-segmentation approaches for PET: report of AAPM task group No. 211. Med Phys 2017; 44: e1-e42.
[16] Niyonkuru A, Chen X, Bakari KH, Wimalarathne DN, Bouhari A, Arnous MMR and Lan X. Evaluation of the diagnostic efficacy of (18) F-Fluorine-2-Deoxy-D-Glucose PET/CT for lung cancer and pulmonary tuberculosis in a Tuberculosis-endemic Country. Cancer Med 2020; 9: 931-942.
[17] Mena E, Sheikhbahaei S, Taghipour M, Jha AK, Vicente E, Xiao J and Subramaniam RM. 18F-FDG PET/CT metabolic tumor volume and intratumoral heterogeneity in pancreatic adenocarcinomas: impact of dual-time point and segmentation methods. Clin Nucl Med 2017; 42: e16-e21.
[18] Paulino AC, Koshy M, Howell R, Schuster D and Davis LW. Comparison of CT- and FDG-PET-defined gross tumor volume in intensity-modulated radiotherapy for head-and-neck cancer. Int J Radiat Oncol Biol Phys 2005; 61: 1385-1392.
[19] Jimenez-Jimenez E, Mateos P, Aymar N, Roncero R, Ortiz I, Gimenez M, Pardo J, Salinas J and Sabater S. Radiotherapy volume delineation using 18F-FDG-PET/CT modifies gross node volume in patients with oesophageal cancer. Clin Transl Oncol 2018; 20: 1460-1466.
[20] Mallak N, Hope TA and Guimaraes AR. PET/MR imaging of the pancreas. Magn Reson Imaging Clin N Am 2018; 26: 345-362.
[21] Liao S, Lan X, Cao G, Yuan H and Zhang Y. Prognostic predictive value of total lesion glycolysis from 18F-FDG PET/CT in post-surgical patients with epithelial ovarian cancer. Clin Nucl Med 2013; 38: 715-720.
[22] Kang B, Lee JM, Song YS, Woo S, Hur BY, Jeon JH and Paeng JC. Added value of integrated whole-body PET/MRI for evaluation of colorectal cancer: comparison with contrast-enhanced MDCT. AJR Am J Roentgenol 2016; 206: W10-20.
[23] Chen BB, Tien YW, Chang MC, Cheng MF, Chang YT, Wu CH, Chen XJ, Kuo TC, Yang SH, Shih IL, Lai HS and Shih TT. PET/MRI in pancreatic and periampullary cancer: correlating diffusion-weighted imaging, MR spectroscopy and glucose metabolic activity with clinical stage and prognosis. Eur J Nucl Med Mol Imaging 2016; 43: 1753-1764.
[24] Lee DH and Lee JM. Whole-body PET/MRI for colorectal cancer staging: is it the way forward? J Magn Reson Imaging 2017; 45: 21-35.
[25] Lee DH, Lee JM, Hur BY, Joo I, Yi NJ, Suh KS, Kang KW and Han JK. Colorectal cancer liver metastases: diagnostic performance and prognostic value of PET/MR imaging. Radiology 2016; 280: 782-792.
[26] Shang K, Cui B, Ma J, Shuai D, Liang Z, Jansen F, Zhou Y, Lu J and Zhao G. Clinical evaluation of whole-body oncologic PET with time-of-flight and point-spread function for the hybrid PET/MR system. Eur J Radiol 2017; 93: 70-75.
[27] Kleeff J, Korc M, Apte M, La Vecchia C, Johnson CD, Biankin AV, Neale RE, Tempero M, Tuveson DA, Hruban RH and Neoptolemos JP. Pancreatic cancer. Nat Rev Dis Primers 2016; 2: 16022.
[28] Chirindel A, Alluri KC, Chaudhry MA, Wahl RL, Pawlik TM, Herman JM and Subramaniam RM. Prognostic value of FDG PET/CT-derived parameters in pancreatic adenocarcinoma at initial PET/CT staging. AJR Am J Roentgenol 2015; 204: 1093-1099.
[29] Lee JW, Kang CM, Choi HJ, Lee WJ, Song SY, Lee JH and Lee JD. Prognostic value of metabolic tumor volume and total lesion glycolysis on preoperative F-18-FDG PET/CT in patients with pancreatic cancer. J Nucl Med 2014; 55: 898-904.
[30] Barral M, Taouli B, Guiu B, Koh DM, Luciani A, Manfredi R, Vilgrain V, Hoeffel C, Kanematsu M and Soyer P. Diffusion-weighted MR imaging of the pancreas: current status and recommendations. Radiology 2015; 274: 45-63.

[31] Kurosawa J, Tawada K, Mikata R, Ishihara T, Tsuyuguchi T, Saito M, Shimofusa R, Yoshitomi H, Ohtsuka M, Miyazaki M and Yokosuka O. Prognostic relevance of apparent diffusion coefficient obtained by diffusion-weighted MRI in pancreatic cancer. J Magn Reson Imaging 2015; 42: 1532-1537.

[32] Ma C, Li J, Boukar MB, Yang P, Wang L, Chen L, Su L, Qu J, Chen SY, Hao Q and Lu JP. Optimized ROI size on ADC measurements of normal pancreas, pancreatic cancer and mass-forming chronic pancreatitis. Oncotarget 2017; 8: 99085-99092.